BNL-114286-2017-TECH

/591; CERN-ACC-NOTE-2018-0039;BNL-114286-2017-IR

SRF cavity testing using a FPGA Self Excited Loop

I. Ben-Zvi

August 2017

Collider Accelerator Department

Brookhaven National Laboratory

U.S. Department of Energy

USDOE Office of Science (SC), Nuclear Physics (NP) (SC-26)

DISCLAIMER

CERN-ACC-NOTE-2018-0039

2018-04-18

ilan.ben-zvi@cern.ch

SRF cavity testing using a FPGA Self Excited Loop

I. Ben-Zvi
BNL, Stony Brook University and CERN

Keywords:

Abstract

This document provides a detailed description of procedures for very-high precision calibration and testing of superconducting RF cavities using digital Low-Level RF (LLRF) electronics based on Field Programmable Gate Arrays (FPGA). The use of a Self-Excited Loop with an innovative procedure for fast turn-on allows the measurement of the forward, reflected and transmitted power from a single port of the directional coupler in front of the cavity, thus eliminating certain measurement errors. Various procedures for measuring the quality factor as a function of cavity fields are described, including a single RF pulse technique. Errors are estimated for the measurements.

Table of Contents

1 Introduction

Various authors have previously studied the theory and practice of cavity testing, notably an extensive treatment by Powers [1] and Padamsee [2]. The advent of the digital Low-Level RF (LLRF) electronics based on Field Programmable Gate Arrays (FPGA) provides various improvements over the rather complex systems used in the past as well as enabling new measurement techniques.

This document is meant to serve as a general guide and specifications document for the operation of the FPGA Self Excited Loop (SEL) operations in testing SRF cavities at CERN (in this context the FPGA refers to the hardware and a particular firmware as developed at CERN). Still, a number of novel methods are presented here, such as the fast start-up, the fast scan and the loop-phase control, discussed further on, as well as extensive error estimates.

The SEL has some advantages for SRF cavity testing. The main one is a rapid set-up of the testing process, it finds the resonant frequency of the cavity within a reasonably wide frequency band, but thanks to the FPGA firmware this band is not too wide to erroneously latch on to a higher frequency mode of the cavity.

Another important advantage is that the SEL tracks well the frequency of the cavity under conditions that the frequency changes, either slowly (cryostat pressure changes) or fast, due to Lorentz detuning or even extremely fast, due to multipacting. Thus, the SEL enables a good fill of the cavity and keeps the best power coupling under the fast-reactive detuning of multipacting electrons, speeding up the conditioning of multipacting.

Another advantage, which will be further discussed in this document, is that the SEL FPGA board measures both In-Phase and In-Quadrature (IQ) components of the RF waveform, and thus acts as a very precise vector voltmeter. This can be used to keep the correct value of the loop-phase and reduce some phase related errors.

A disadvantage is the ability of the SEL to lock on an unintended frequency if it is close to the target mode, for example in the accelerating pass-band of a multi-cell cavity. Thus, one should check the frequency selected by the SEL.

Another potential disadvantage is that the turn-on (sending full forward power) of the SEL can be slow since it takes time for the SEL to establish the oscillation and the loop-phase. This is when the SEL has to start from noise. However, as we have established in tests carried out at CERN's SM18, applying a two-step process resolves this issue nicely. In this process the SEL is started at a low level, say at a fraction ε of the intended voltage (represented on the board by a DAC word) for a brief time (please see Section 5.4.3.1 for analysis of this ε). At this low level and short on-time the cavity stores a negligible amount of energy. Then, with the SEL oscillating at the right frequency and loop-phase, the forward power is switched on to the full-required level. The cavity is then practically empty of stored energy, and the reflected power port indicates the full forward power reflected off an empty cavity. This makes a precise measurement of the coupling coefficient β as well as the cavity absorbed power possible.

An advantage of the FPGA LLRF system is the accurate and highly linear measurement of the RF signal voltage using high precision Analog to Digital Converters (ADCs) to quantify the input signals.

In this document we reintroduce a technique that seems to have fallen out of practice in recent times, that is obtaining the coupling constant β through measurements from just one port, the reflected power port, of the directional coupler placed in front of the cavity.

2 The SEL circuit

A disclaimer: Some of the specific features of the circuit and firmware described here are representative of the SEL FPGA board used by the CERN SRF group at SM18, other FPGA boards probably have different features, however the general principles still hold.

A schematic diagram of the main elements of the SEL is given in Figure 1. Two signal generators are connected to the SEL board. These are the Local Oscillator, (marked LO) and the Sampling Rate (marked SR). The LO has to be set to provide the down-conversion of the frequencies to the Intermediate Frequency (IF) of the SEL, which is about 20 MHz. The exact value of the IF can vary around 20 MHz. The choice of the LO frequency has to be a rational fraction of the cavity frequency, such as 19/20, 29/30 and so on. Thus, the IF frequency is set to 1/20, 1/30 and so on of the cavity frequency, close to 20 MHz. Then the SR oscillator has to be set to exactly 4 times the IF frequency. The maximum IF frequency is 30 MHz.

The two signal generators should be synchronized, with a cable connecting the frequency reference (usually on the back panel of the devices) from one to the other.
When the frequency of the LO and SR are changed, the FPGA board should be switched off and then back on, to certain registers which are set to remember this frequency at power-on.

The FPGA uses ADCs and DACs with a typical number of voltage level, represented by a binary word of up to about 20,000. The voltage should be kept at or below 20,000 to allow sufficient headroom for digital operations on the board. However, it should be large compared to the ADC noise floor at ADC/DAC counts to obtain a good dynamic range.

The FPGA deals with RF voltage waveforms, which is the correct way to handle RF circuits. The RF signals we transmit and process are forward and reflected voltage and current waves in transmission lines, each with a phase depending on the time and position of the measurement. Mixing of RF waveforms always takes place as a linear superposition of the voltages and currents, and not of the power levels that can be assigned to these waveforms. It has to be understood that when we talk about RF power for convenience, it is just a particular measure of the properties of the electromagnetic waves.

Within the SEL board, the incoming RF signals (characterized by an amplitude and phase relative to some reference) are amplified, filtered and down-converted to the IF frequency using double-balanced mixers. The signals are then digitized by ADCs at the sampling rate of four times the IF frequency, thus one gets the zero, in-phase zero and in-quadrature values at each RF cycle. These digitized signals are processed by the FPGA and then up-converted back to the original RF frequency. The presentation of results can be made as I-Q (In-phase and in-Quadrature) components of the RF signal or converted to amplitude and phase. One has to be careful when transforming the voltages measured on the board to power, which is the favorite output format.

Thanks to the specific choice of LO and SR frequencies, the board possesses a “virtual frequency” which is the intended cavity frequency. If the RF signal that is digitized has a different frequency, it will be tracked as a vector rotating relative to this virtual frequency, at a rotation rate that is the difference between the virtual frequency and the measured RF frequency. The board measures this difference-frequency, so that at any time the circuit can provide an instantaneous reading of the frequency of the SEL.

There are other ports in the SEL board, which can be used for checking on the board settings, but these will not be discussed in this document.

We would like to make clarifying remark concerning the interpretation of power and voltage. The cavity input line and transmitted power line as well as other are RF power transmission lines. Normally one considers power as a scalar. However, in the context of this work, the power in the transmission line is associated with an RF voltage, which has a phase and is thus a vector, as described above. The RF input lines are converted by ADCs into voltages, and the phase is captured as mentioned earlier by taking both in-phase and in quadrature components of the signal. While the FPGA is operated with digital words containing the in-phase (I) and in-quadrature (Q) components of each voltage data point, these can also output as amplitude and phase.

Since the communication of the operator with the SEL is digital, through data lines, the board can and should be placed as close to the cavity as possible (whilst considering, for example, issues of damaging radiation from the cavity or temperature stability). This is to reduce noise and potential phase drifts due to temperature changes of the connecting cables.

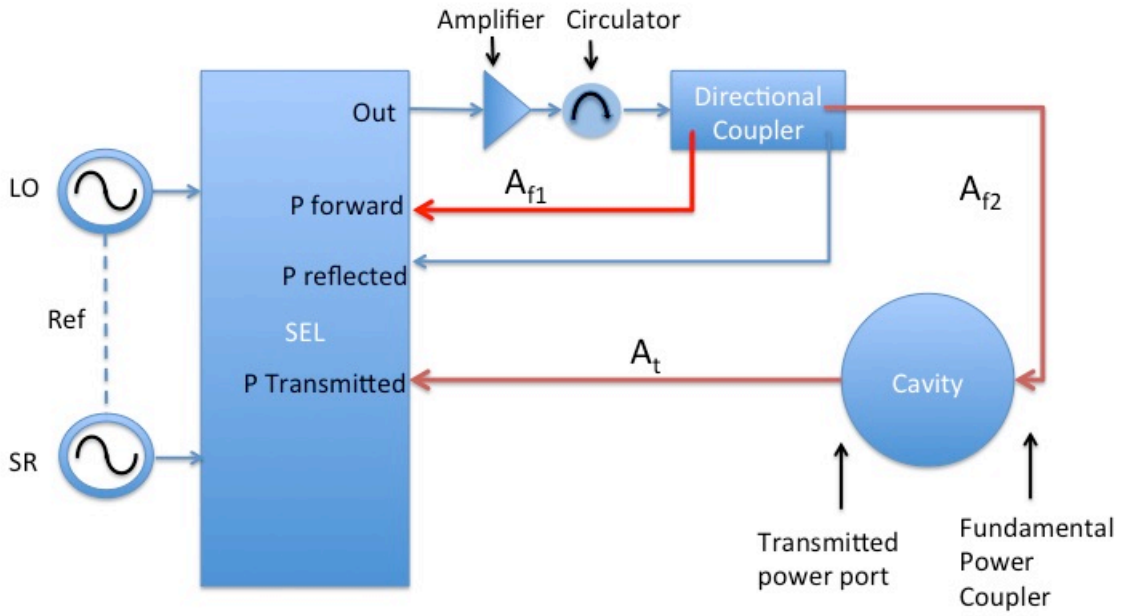

Figure 1. A schematic diagram of the main elements of the SEL. Lines in bold-red (marked A_{f1} , A_{f2} and A_t require precise calibration, A_{f1} includes the coupling factor of the directional coupler). LO and SR are signal generators providing the Local Oscillator frequency and the Sampling Rate, and they are connected with a common reference (dashed line).

2.1 Calibration of peripherals.

The digital numbers in the ADCs or DACs refer to voltage levels, not power. The input power P (in watts), corresponding to the ADC digital word W is given as $P = W^2/N$, where N was measured at one time to be about $N = 2.5424*10^{10}$, where the power in Watts P.

This number should be checked periodically since we observed a non-negligible change in the N value over a period of one month.

The linearity of the ADCs W^2 vs. power is excellent over the measured range of over 20,000. The calibration factor N is used to convert the SEL board digital voltages to actual power at the SEL terminals. An ADC count of 20,000 is about 15.7 mW with the given N. Since the ADCs have 16 bits of digitization range, an ADC count of 20,000 is safely within the ADC range.

The SEL terminals are connected to the two main cavity ports through RF cables with particular attenuation values. The first port is the forward power terminal of the directional coupler connected between the RF amplifier (and its circulator) and the cavity. The other port is the pickup antenna measuring the transmitted power from the cavity. A calibration of the cables A_{f1}, A_{f2} and A_t is critical for the precise calibration of the conversion coefficients Q_L and Q_t (external Qs of the FPC and transmitted power coupler, respectively) for precise measurements of the cavity's stored energy U and quality factor Q_0.

Please note that the A_{f1} attenuation presented in Figure 1 and used in this section must include the port coupling of the coupler, which is treated as a large equivalent attenuation due to the weak coupling of the port.

It must be emphasized that the directional coupler has to be of the highest quality in terms of isolation (see section 5.4.2.3 for details). The location of the directional coupler should be as close to the cavity as possible, ideally on the top-plate of the cryostat. This is important to reduce the effect of the phase drift introduced by the RF cable between the directional coupler and the FPC. The length of this cable and that of the cable connected to the transmitted power pickup antenna, both of which are inside the cryostat, should be selected to have a low temperature coefficient.

The RF cables between the cavity and the SEL should be kept short considering shielding constraints, in order to reduce the effect of the Lorentz detuning on the phase change across the cables. In addition, ideally, they should have as few as possible breaks (e.g. for additional directional couplers for other purposes than the circuit of Figure 1). In addition, these runs of cables for the forward power reading from the directional coupler and the transmitted power antenna should be of approximately the same length and should be routed together to experience the same temperature profile. In addition, any devices inserted in these lines, such as power splitters or directional couplers should be paired with similar devices in the other line, placed in the same location. However, as said earlier, it is best to avoid any avoidable insertions, and the cables should be made of as few sections as possible, to avoid multiple reflections.

The circulator shown in Figure 1 is an important element to be placed after the amplifier and before the directional coupler. The amplifier port usually has a poor match and produces a reflection of power incident upon it. Thus, without a circulator, a signal reflected from the cavity can be reflected back from the amplifier and combine with the forward power from the amplifier with a phase that depends on the delay of the cables, leading to an erroneous measurement of the forward power by the directional coupler. Thus, the match of the circulator, in particular for the coupled port, has to be very good (see section 5.4.2.4 for details).

A simple test can be carried out to check the quality of both directional coupler and isolator. Using a constant power from the amplifier, the loop-phase can be stepped by a significant amount (say 30 degrees) symmetrically to either side of the optimal loop-phase, observing the forward power reading from the directional coupler. If this reading is different for the two loop-phase settings, then there is a non-negligible error due either to the isolation of the directional coupler or the reflection from the cavity-side port of the circulator.

Another port that is critical for the measurement is the reflected power port of the directional coupler. In the measurement scheme described in this document, an absolutely precise measurement of the attenuation of this cable is not important. An a-priori knowledge of the strength of the coupling (overcoupled or undercoupled) is also not necessary, since the method given here determines unambiguously the degree of coupling β. This is quite unlike the conventional method, which establishes the power going into the cavity by a subtraction of the carefully calibrated signals of the forward and reflected power from the directional coupler, a practice that more than doubles the measurement error *ceteris paribus*.

A criterion for choosing the directional coupler coupling strength is to keep the RF signals at which measurements take place well above the digital noise in the FPGA board. This is important for both the transmitted power and the reflected power measurement, and to some extent also the forward power measurement. Thus the attenuation of the cables, including the coupling coefficients of the directional coupler should be chosen carefully to avoid small digital numbers from the ADCs at the low stored energy range of the measurement, in particular the calibration.

At the same time, one should avoid digital words that are too large, say over 20,000, to allow for computational headroom in the FPGA. It is always better to add fixed precision attenuators if the signal level becomes too high; the use of RF amplifiers in the measured cavity signals is to be avoided due to phase drifts, noise and non-linear terms.

Now we address the calibration of the absolute power related to the $\mathbf{P_f}$ and $\mathbf{P_t}$ read by the forward and transmitted ADC ports, respectively. Let us accept that the cable attenuations A_{f1}, A_{f2} and A_t are given in dB. Thus, the absolute forward power as seen by the cavity $\mathbf{P_f}$ (bold face marking that this is the real power on the FPC port) is given in watts by:

$$\boldsymbol{P_f} = \frac{W_f^2}{N} 10^{0.1(A_{f1} - A_{f2})}$$

Where W_f is the digital number read by the forward power ADC. Since the SEL board maintains both amplitude and phase or the I-Q values of each voltage, here we are considering W_f to be the amplitude (not the in-phase or in-quadrature values).

The cavity sees a power smaller by A_{t2} than that measured at the forward port of the directional coupler, thus A_{f2} has to be subtracted from A_{f1}.
Similarly, the real transmitted power at the pickup antenna is given by

$$\boldsymbol{P_t} = \frac{W_t^2}{N} 10^{0.1A_t}$$

Where W_t is the digital number read by the transmitted power ADC.

3 SEL operating sequences

3.1 Introduction to operations

The preparation to operations must start with the calibration of the peripherals as described in Section 2.1 above. The measured attenuations (marked in Figure 1) are entered into the software database for use in calculations.

In this document when we discuss a pulsed operation, it must be understood that we require a short pedestal pulse at a very low power level to precede the actual pulse turn-on. This is done in order to allow the SEL circuit to lock on the cavity at the right phase and allow a sharp leading edge of the actual pulse. The quantification of "short" and "very low power" are given in Section 5.4.3.1.

Next we must assure that the SEL is operating at exactly the resonant frequency of the cavity, or equivalently, that the phase difference between the incident RF power and the transmitted RF power at the cavity is exactly zero. Since the length of cables and the phase shift introduced by amplifiers can drift with time and temperature change, it is critical to verify this condition for each measurement by doing a phase-scan. The phase-scan should avoid hitting a multipacting barrier or using ADC words which are too small for precision. We will designate this parameter as Ψ_0. It will be used as a reference to correct phase drifts.

The procedure for a phase-scan is to step the loop-phase of the SEL board at a constant forward power and maximize the transmitted power. There is no need to start the scan with a fine phase step since the peak is quite wide. Once the approximate location of the peak in the transmitted power is found, a narrow phase-range can be scanned with increased resolution to establish the exact setting of the loop-phase.

The seven quantities that we expect to get from the FPGA board for the cavity calibration and test sequences are as follows:

1. The decay time τ of the stored energy of the cavity when no power is applied. This is essentially a measurement of the loaded Q (Q_L) of the cavity, or equivalently a measurement of the width of the resonance curve. The SEL board actually measures voltages, thus it is important to remember that the voltage decay time is twice as long as the power decay time.
2. The forward power $\mathbf{P_f}$ as seen by the cavity. This is obtained from the measured forward power port of the directional coupler, with cable calibration factors as described in the previous section. This quantity is presented as both in-phase voltage and in-quadrature voltage (I-Q), thus it is a vector (I,Q) or an amplitude and a phase.
3. The transmitted power from the cavity $\mathbf{P_t}$, with cable calibration factors as described in the previous section. This is a voltage vector.
4-6. The power levels (the SEL actually measures voltages) of the reflected power port, P_a, P_b and P_c, as depicted in Figure 2 and described in Appendix 1. These are also I-Q voltage vectors on the board.
7. The frequency of the closed SEL loop. This last quantity is used in CW scans.

The following remarks are important. The measurement of the decay time is not trivial when the intrinsic Q of the cavity is a function of the stored energy, which is naturally what we aim to measure. On one hand, from the mathematical point of view, one tends to measure the decay over a good fraction of the expected decay time for a good accuracy, but then the decay curve deviates from an exponential function due to the change in Q. Thus, one should fit the exponential decay over the shortest time that still provides a precise value for the decay time. Each value of τ must be matched to the relevant value of the stored energy (or transmitted power).

Given that the SEL board provides measurements of the decay of the stored energy at constant (very small) intervals Δt, we obtain $\tau(t)$ from the transmitted power decay curve as

$$\tau(t) = \frac{-P_t(t)}{dP_t(t)/dt}$$

However, since the digital noise in the FPGA is constant, for a small Δt the derivative of $\mathbf{P_t}$ would be catastrophically noisy, thus a polynomial fit of $P_t(t)$ must be done before this function is evaluated. Please note that the decay time is a function of the stored energy since the cavity losses are a function of the stored energy. The use of the time variable to fit the decay time is just a matter of convenience.

We define a new variable, Ψ, to be the phase difference $\psi_f - \psi_t$ measured by the FPGA between $\mathbf{P_f}$ and $\mathbf{P_t}$ relative to Ψ_0:

$$\psi \equiv \psi_f - \psi_t - \psi_0$$

Following the phase-scan, the value of this ψ should be recorded for frequent phase drift checks. When the SEL oscillates exactly at the cavity resonant frequency, Ψ should be 0, unless the RF transmission lines from the cavity to the SEL board changed their relative length. Since there are no amplifiers in these lines and the cables are of the same length, the same temperature coefficients and the same environment relative to temperature, we expect this to be a stable indicator. The only drift that is not corrected by this technique is that of the cable between the directional coupler and the FPC and between the transmitted power antenna and the top of the cryostat. If the directional coupler is placed on top of the cryostat, these are relatively short cables and should also be chosen to have a low temperature coefficient.

Note that only ratios of P_a, P_b and P_c are used in the procedures described in this document, thus a precise cable calibration of the reflected power port of the directional coupler is not necessary.

3.2 The cavity's couplers calibration sequence

The objective of a cavity calibration sequence is the measurement of the external coupling of the two ports, the external quality factor Q_e of the Fundamental Power Coupler, and external quality factor Q_t of the pickup antenna.

Ultimately, the objective of measuring a cavity is to determine it stored energy U and intrinsic quality factor Q_0 at various values of U. Given that the connection from the exterior of the cavity to its interior is conducted through coupling ports, then it is clear why it is necessary to determine the properties of these ports.

The power level for the calibration should be chosen carefully (see further down). The τ fit error (measuring its deviation from a perfect exponential decay) at and just under the start of the decay of stored energy (just as the forward power is turned off) is a good indicator for the quality of the fit. The loop-phase must be optimized before a calibration.

Decay time measurements are inherently very precise. The procedure is to follow the decay of the transmitted power from the moment the forward power has been switched off over about one exponential decay and calculate a best fit of the measured points to an exponential decay. The best-fit procedure provides an error, which is typically about 10^{-5}, that is much more precise than anything else in the measurement.

The best-fit quality may become bad if the decay measurement is extended over a stored energy range in which there is a significant change in the quality factor of the cavity. Such a change can occur due to a large Q-slope, onset of multipacting or field emission. Thus, one should follow the measurement of $\tau(t)$ and best fit procedure outlined above.

We use the following common definitions:

$$\beta \equiv \frac{Q_0}{Q_e}$$

where Q_0 is the quality factor of the bare cavity and Q_e is the external Q of the FPC and

$$\beta_t \equiv \frac{Q_0}{Q_t}$$

where Q_t is the external quality factor of the transmitted power antenna.

As a reminder, in the following we use as inputs six of the values measured by the FPGA board as described above in Section 3.1: τ, $\mathbf{P_f}$, $\mathbf{P_t}$, P_a, P_b and P_c. The seventh quantity, the frequency of the SEL, is not used in the calibration. The bold face serves as a reminder that those quantities have been corrected for cable and device attenuation, and they are also vectors (amplitude and phase). We aim to extract Q_e and Q_t, the products of the calibration.

In the following we are not assuming that the transmitted antenna coupler can be neglected in the extraction of the FPC coupling from the measurements.

Before a calibration, a phase-scan must be done and Ψ (defined above in Section 3.1) is verified to be zero.

Therefore, the calibration procedure is as follows:

1. Send a pulse (preceded by a pedestal) of sufficient length, at least 10 decay times).
2. Measure $\mathbf{P_f}$, $\mathbf{P_t}$, P_a, P_b and P_c. Verify that $\Psi=0$.
3. Obtain τ from a best fit of the decay $e^{-t/\tau}$ of the transmitted power. As described above, τ is a function of the stored energy in the cavity and thus we choose the value of τ at the stored energy representing the calibration point. Publish τ and the error. Set alarm to discard this result if the error exceeds a set level. The decay time is a measure of the loaded Q of the cavity, Q_L:
$$Q_L = \omega\tau$$

4. Calculate β as

$$\beta = \frac{P_c}{P_a(1-\epsilon) - P_b}$$

where

$$\epsilon \equiv \left| \boldsymbol{P_t} \middle/ \boldsymbol{P_f} \right|$$

5. Calculate β_t as

$$\beta_t = \beta\epsilon\frac{P_a}{P_c}$$

(See Section 5.2 as well as Figure 2 for the definition of these variables and derivations of expressions). Often the term $\mathbf{P_t/P_f}$ can be neglected when Q_t is orders of magnitude larger than Q_e, but we do not neglect it in this work.

Also obtain statistical errors on P_a, P_b and P_c for error calculations.

6. **Obtain Q_e,** the external Q for the FPC, from

$$Q_e = \frac{1+\beta+\beta_t}{\beta}\omega\tau$$

Save this Q_e value for use in scans, this is one of the two main calibration results, used in scans to calculate Q_0. This Q_e is a geometrical quantity fixed for this probe, which changes only of this coupler is replaced or perturbed.

7. **Obtain Q_t** from

$$Q_t = \frac{1+\beta+\beta_t}{\beta_t}\omega\tau$$

8. **Obtain α** defined as

$$\alpha = \left| \boldsymbol{P_f} \middle/ P_a \right|$$

This constant will be used in a CW scan sequence.

Note that to get the external quality factor of the pickup antenna, which is a geometrical quantity for this coupler, is the second of the two objectives of the calibration process. Q_t is often replaced by a different constant, $K = Q_t/\omega$. K is used to obtain the stored energy in scans through $U = K\mathbf{P_t}$, and hence to get the voltage or gradient of the cavity for Q_0 vs. voltage / gradient plots.

Apart from the calibration, we also get the stored energy U and Q_0 from

$$Q_0 = (1+\beta+\beta_t)Q_L \;;\; U = K\boldsymbol{P_t}$$

These values and the errors in τ, Q_e and Q_t should be published as part of the calibration to record the conditions at the point of the calibration. However, plots of U and Q_0 are obtained in scans, which use the results of the calibration. The stored energy is related to the voltage or gradient of the cavity through

$U = \kappa V^2$, where the coefficient κ is obtained by an electromagnetic solver program (e.g. Superfish, Microwave Studio etc.).

We also get P_0 (power absorbed by cavity) from

$$P_0 = \boldsymbol{P_f}\frac{P_a - P_b}{P_a} - \boldsymbol{P_t} = \boldsymbol{P_f} - \alpha P_b - \boldsymbol{P_t}$$

Repeating the above-mentioned notes of caution: For a good cavity calibration, the loop phase must be set correctly by maximizing the P_t and / or minimizing P_r as a function of loop phase before the calibration is done, and the measurement of τ must be made in a clean exponential decay of the stored energy otherwise the results will be in error.

Note also that the method used here (item 1) of determining β does not require an a-priori knowledge if the port is undercoupled or overcoupled, and it does not require a precise calibration of the reflected power circuit, since in all cases we use just ratios of two quantities measured at this port. Therefore, this technique is quite precise and less prone to calibration errors. This concludes the calibration sequence.

Variable Coupler: As an aside, we would like to mention the advantages gained if a variable coupler is available for the test of the cavity. With a variable FPC, the calibration sequence is greatly simplified as well as the errors are reduced:

1. Send a pulse (preceded by a pedestal) of sufficient length, at least 10 decay times).
2. Measure $\mathbf{P_f}$, $\mathbf{P_t}$, P_a, P_b and P_c. Verify that Ψ=0.
3. Adjust the coupler to null the reflected power P_b, thus P_c=P_a and
$$\beta = \frac{1}{1-\epsilon}$$
where we defined $\epsilon = \boldsymbol{P_t}/\boldsymbol{P_f}$ to stress that usually it is a small quantity.
4. Obtain τ from a best fit of the decay $e^{-t/\tau}$ of the transmitted power (described earlier) at the stored energy corresponding to the filled cavity at the given forward power.
$$Q_L = \omega\tau$$
5. Obtain β_t from
$$\beta_t = \frac{\epsilon}{1-\epsilon}$$
6. **Obtain $\boldsymbol{Q_e}$,** the external Q for the FPC, from
$$Q_e = 2\omega\tau$$
7. **Obtain $\boldsymbol{Q_t}$** from
$$Q_t = \frac{2\omega\tau}{\epsilon}$$

3.3 The pulsed scan sequence

Once the calibration is done, one may proceed to measure the Q vs. stored energy (meaning either the voltage or field) curve of the cavity. This process is referred to as a scan; the quality factor is measured as the stored energy (i.e. field or voltage) of the cavity is scanned over a given range. This process may be carried out in a pulsed scan, as described in this section, or in a CW scan, as described in the following Section 3.4. The main advantage of a pulsed scan is the ability to reduce the average power in the cavity, due to the less than unity duty factor. The main disadvantage is that the cavity has to be filled and then emptied of stored energy, which is somewhat time consuming.

During a pulsed scan, at any one of a set of forward power levels, the following steps are taken:

1. Send a pulse (preceded by a pedestal) of sufficient length, at least 10 decay times).
2. Measure $\mathbf{P_f}$, $\mathbf{P_t}$, P_a, P_b and P_c. Verify that $\Psi=0$.
3. Obtain measured values of τ and P_t (τ is obtained from the fitting as above, set alarm if error of fit exceeds limit)
   Note that τ is a function of voltage, so one should obtain the fitted value of τ over a short time interval near the voltage of the steady state.

4. Calculate $U = K\boldsymbol{P_t}$ where $\boldsymbol{P_t}$ is measured, and K is in the results of the calibration, then derive the voltage (or gradient) from $V = \sqrt{\frac{U}{\kappa}}$

5. Calculate

$$Q_0 = \frac{1}{\frac{1}{\omega\tau} - \frac{1}{Q_e} - \frac{1}{Q_t}}$$

where Q_e and Q_t are results of the calibration and τ is measured.

6. Check that $\Psi=0$, else change the loop-phase to null Ψ.

The main product of the scan is a plot Q_0 vs. V

It is also interesting to get the power absorbed by the cavity,

$$P_0 = \boldsymbol{P_f}\frac{P_a - P_b}{P_a} - \boldsymbol{P_t} = \boldsymbol{P_f} - \alpha P_b - \boldsymbol{P_t}$$

3.4 The CW scan sequence

The main advantage of this scan method is its ability to optimize the loop-phase continuously throughout the measurement, contributing to precision of the measurement and immunity to slow phase drifts of the system. Another advantage is that is can be done faster, since one avoids the pulse off periods as well as the need to refill the full energy content of the cavity.

The scan is carried out over a range of forward power values. The power is stepped to a new value without turning off the SEL, and then that value is maintained for the duration required to establish the transmitted power and the loaded Q. At each point of the scan (defined by the forward power), we

perform a square-wave modulation of the loop phase φ, such that φ = ±φ_0. Note that the unit for the phase is radians, not degrees. The alternation of the phase must be done once in 9τ or longer, to allow the cavity loop to settle and get a precise measurement.
Measure the following:

1. **P_t**, which provides U through K obtained in the calibration.
2. Q_L, which provides Q_0 as described in the pulsed scan sequence, Section 3.3.

To measure Q_L, measure the frequency deviation δ_f corresponding to the loop phase modulation φ. Then, using the expressions from Appendix 2, the frequency will be modulated with an amplitude of $\delta_f = f\varphi_0/2Q_L$. Thus, we derive

$$Q_L = \frac{f\varphi_0}{2\delta_f}$$

The data from the SEL is δ_f, and since f is known and φ_0 is set by us, we know Q_L.

So the sequence is as follows: Arrive at a new power level. Wait sufficiently for the stored energy and frequency to settle. Record the stored energy and frequency. Now start modulating the phase. Step the loop-phase to $-\varphi_0$. Wait for f to settle. Record f, switch phase to φ_0. Repeat if necessary to take advantage of averaging.

Calculate Q_L as described above; now check the phase setting as described below.

To check the exact zero phase of the loop, normally we measure Ψ.

However, the asymmetry of the amplitude of the transmitted voltage under phase modulation φ is also a measure of Ψ. We get the offset Ψ also through:

$$\psi = -\frac{1}{2\varphi}\frac{V_t^+ - V_t^-}{V_t^+ + V_t^-}$$

Here $V_t^+ \; and \; V_t^-$ correspond to the amplitude of the transmitted voltage corresponding to a step $\pm\varphi_0$.

To reduce the noise, the modulation is carried out M times (for both positive and negative values of Φ), and the results are averaged out to reduce the noise.

The intrinsic quality factor Q_0 and the stored energy are then obtained through

$$Q_0 = \frac{1}{\frac{1}{Q_L} - \frac{1}{Q_e} - \frac{1}{Q_t}}$$

and

$$U = K\boldsymbol{P_t}$$

Usually the desired quantity to plot is the voltage (or gradient) of the cavity, given by $V = (U/\kappa)^{0.5}$.

The power absorbed by the cavity is simply $P_0 = UQ_0/\omega$

3.5 Quick loop-phase correction

Once the coarse phase-scan of the cavity has been established and the loop-phase has been set to its optimum value (maximize U as a function of loop-phase), the phase deviations are expected to be small, and we keep track of drifts by monitoring Ψ. However, we can check on how good Ψ is using the following method for quick loop-phase correction, to undo phase drifts in Ψ. The procedure described above in Section 3.4 for correcting the phase can be applied, even in a pulsed-scan or just for verification:

$$\psi = -\frac{1}{2\varphi}\frac{V_t^+ - V_t^-}{V_t^+ + V_t^-}$$

4 Fast alternate scan sequences

At various points we stressed the need to wait a sufficient time for the cavity's stored energy to stabilize (in amplitude and frequency, either full or empty). In Section 5.4.3.1 we analyzed the errors introduced into the various measured quantities the finite fill (or empty) times. To reduce these errors, it is necessary to wait long periods of time in the pulse-on or pulse-off situations. This is certainly the case for a calibration sequence. A scan takes many measurement points. However, with very good quality factors these waiting times can be on the order of many seconds for each point in the scan. Here we propose a method that can reduce these waiting times by making proper corrections. We will do so by noting that the fill errors (Section 5.4.3.1) are predictable, and thus correctable.

4.1 Fast pulsed scan sequence

We proceed through a set of forward power levels, exactly as described in Section 3.3 above. The pulse "on" time and "off" time can be of the order of a decay time τ, thus the cavity will not fill to the saturation value corresponding to the applied forward power, thus the value of $\mathbf{P_t}$ is taken just at the end of the power-on period, and the stored energy at that point is still given by

$$U = K\boldsymbol{P_t}$$

The decay time is measured as described in Section 3.3, and thus yields the Q_0 in the same way.

Therefore, the pulsed scan can be done relatively fast, with each stored energy point taking time about the order of 2τ. There is no need to wait for draining all the energy of the cavity and the forward power can be set to a high value to speed up the charging curve. The procedure then stops the forward power just as the transmitted power reaches the desired value.

4.1.1 Single-pulse Q vs. V scan.

An even faster scan can be made in a single pulse.

Fast scan measurement methods can yield Q vs. V curves that show hysteresis if there are significant surface heating effects at particular defects. Since the heating (or cooling) of such a "bad spot" may be slower than the scan speed, the Q vs. V may depend on the speed of the scan. This effect would be more pronounced at higher voltages.

Since the voltage build-up and decay curves contain information about the decay rate continuously at any point, the decay rate can be extracted as a function of stored energy, obtaining the full Q vs. V curve in a single pulse. The resolution in V depends on the data quality, determining how short a segment is sufficient to extract the local decay time with sufficient precision.

Scan on voltage build-up using the transmitted power

We have seen that on resonance, the on-resonance stored energy varies along the power pulse like

$$U = \frac{4\beta \boldsymbol{P_f} \tau}{1+\beta}\left(1 - e^{-t/2\tau}\right)^2 = \frac{4\boldsymbol{P_f}\omega}{Q_e}\tau^2\left(1 - e^{-t/2\tau}\right)^2$$

or the voltage follows

$$V = \sqrt{\frac{\boldsymbol{P_f}\omega}{Q_e}}\tau\left(1 - e^{-t/2\tau}\right)$$

Therefore, one can fit the function $\left(1 - e^{-t/2\tau}\right)$ to small segments of the transmitted voltage vs. time curve during cavity voltage buildup and obtain the local value of τ. Since τ provides the value of Q_L, and Q_L leads to Q_0, then this procedure leads to a Q_0 vs. V curve in a single pulse during the voltage build-up phase.

Scan on voltage build-up using the reflected power

The reflected voltage follows the functional dependence of the reflection coefficient, given in Section 5.1 Eq. 5.7b:

$$\Gamma \equiv \frac{V_r}{V_f} = \frac{I_r}{I_f} = 1 - \frac{2\beta}{1+\beta}\frac{1 - e^{-t/2\tau}}{1 + j\delta}$$

Which can be rewritten as:

$$\Gamma = 1 - \frac{2\omega\tau}{Q_e}\left(1 - e^{-t/2\tau}\right)$$

Thus, we can also fit the time constant τ by measuring Γ (or the reflected voltage) on resonance as a function of time during the buildup of voltage in the resonator.

Note that τ is a function of voltage, so one should obtain the fitted value of τ over a short time interval.

Scan on voltage decay

The time constant of the cavity as a function of cavity voltage can also be measured during the free decay by fitting τ to the curve of the amplitude of the transmitted power as a function of time.

$$V_t = V_t^0 e^{-t/2\tau}$$

Note that τ is a function of voltage, so one should obtain the fitted value of τ over a short time interval.

4.2 Fast CW scan sequence

Reflected power based fast CW scan

A fast CW scan can be made if the reflected power can be precisely calibrated relative to the forward power. Then the power absorbed by the cavity can be established by subtracting the calibrated reflected power and transmitted power from the forward power. Since the stored energy is known from the measurement of the transmitted power, then Q_0 can be established through

$$Q_0 = \frac{U\omega}{P_0}$$

Here we use the constant α established in the calibration sequence:

$$P_0 = \boldsymbol{P_f} - \alpha P_b - \boldsymbol{P_t}$$

The stored energy is obtained as usual through

$$U = K\boldsymbol{P_t}$$

Frequency based fast scan

There is a faster alternate sequence for the frequency-based CW scan. In this sequence, we assume that the frequency measured by the SEL FPGA is accurate enough to avoid averaging. The calculation of the stored energy from $\mathbf{P_t}$ is unchanged. However, when we step the loop-phase by φ, the stored energy at the given frequency starts decaying with the decay time τ, and the new frequency, corresponding to the new value of the phase shift starts building up with the same time constant. The energy of the two modes will be equal after an interval $\Delta t = \tau \ln 2 = 0.693\tau$, thus the frequency shift will assume half of the final value, as described in Section 5.2:

Track the frequency output ω(t) from the SEL as a function of time t from the application of the phase jump φ. At some point t_1 in time the following equation will be satisfied by the measured frequency:

$$\frac{\varphi ln2}{4(\omega(t_1) - \omega_0)} = t_1$$

At this point we have established a self-consistent value for τ and thus for Q_L:

$$\tau = \frac{t_1}{ln2}$$

$$Q_L = \omega\tau = \frac{\omega t_1}{ln2}$$

5 Appendix

5.1 The derivation of the basic equations

It is useful to derive the basic equations of a resonator that are used in this document.

Consider an equivalent circuit of a cavity coupled to a transmission line with impedance Z_0. The resistance R, inductance L and capacitance C are connected in series to the terminals of the transmission line through a matching transformer with a turn ration of n:1. At the resonator side of the transformer the currents are n times lower, and the transmission line impedance appears as n^2 times higher. Thus at the circuit the transmission line contributes a series resistance $Z = n^2 Z_0$ to the resonator's intrinsic resistance R

First let us solve the time dependent evolution of the current I through the series circuit, driven by a current V. For the basic RF time dependence, we use a sinusoidal time dependence of the current and voltages of the form

$$u(t) = u_0 e^{-j\omega t}$$

The total voltage across the resonator is the sum of the voltages across the components:

Eq. 5.1 $$V = IR + L\dot{I} + \frac{1}{C}\int I dt$$

In the limit of Z=0, the resistance R represents the intrinsic resistive loss in the resonator.

Differentiation with respect to time is represented by a dot.

Now let us add to the circuit the transmission line that couples current into the resonator.

There are two waves in the transmission line, a forward wave traveling towards the resonator and a reflected wave. We will designate the forward and reflected currents and voltages by a subscript f and r, whereas the resonator current and voltage have no subscript.

Thus, we have the following equations, for the current and voltage at the junction of the transmission line and the resonator:

Eq. 5.2 $$I_f - I_r = I$$

Eq. 5.3 $$V_f + V_r = V = Z\left(I_f + I_r\right)$$

We got 3 equations with three unknowns – I, V and I_r. I_f is a given constant, related to the forward power.

Let us introduce a few definitions:

$$\omega_0 \equiv \sqrt{\frac{1}{LC}};\ \tau \equiv \frac{L}{R+Z};\ \ Q_0 \equiv \frac{L\omega_0}{R};\ \ Q_e \equiv \frac{L\omega_0}{Z};\ \ \beta \equiv \frac{Z}{R} = \frac{Z_0}{Rn^2};\ \ Q_L \equiv \frac{Q_0}{(1+\beta)} = \omega_0\tau$$

We can eliminate the voltage from the differential equation Eq. 5.1 by using the transmission line equations Eq. 5.2 and Eq. 5.3

$$V = Z\left(2I_f - I\right)$$

Substituting V into Eq. 5.1, we get

$$2ZI_f = I(R+Z) + L\dot{I} + \frac{1}{C}\int Idt$$

We differentiate both sides of this equation and divide by L to get (with the above definitions)

$$-j2ZI_f\frac{\omega}{L} = \ddot{I} + \dot{I}\frac{R+Z}{L} + \frac{I}{LC}$$

Using the definitions, we have

$$-j2ZI_f\frac{\omega}{L} = \ddot{I} + \frac{\dot{I}\omega}{Q_L} + \omega_0^2 I$$

Following the differentiation of the current on the right hand side:

$$-j2ZI_f\frac{\omega}{L} = I\left(-\omega^2 - \frac{j\omega^2}{Q_L} + \omega_0^2\right)$$

Let us define: $\Delta \equiv 1 - \frac{\omega^2}{\omega_0^2} \approx 2\frac{\omega_0-\omega}{\omega_0}$; $\quad \delta \equiv Q_L\Delta$

Now we got the solution of the inhomogeneous equation (Eq. 5.1):

Eq. 5.4 $$I = \frac{2\beta}{1+\beta}\frac{I_f}{1+j\delta}$$

Eq. 5.4, with the implicit time dependence of $e^{-j\omega t}$, is the steady state solution for a given forward current.

For the complete solution of the set of equations Eq. 5.1, Eq. 5.2 Eq. 5.3 we should add a solution of the homogeneous equation

$$\ddot{I} + \frac{\dot{I}\omega_0}{Q_L} + \omega_0^2 I = 0$$

It can readily be seen that this equation is satisfied at a frequency $\omega = \sqrt{\omega_0^2 - \frac{1}{(2\tau)^2}}$ by

$$I = I_h e^{-j\omega t - t/2\tau}$$

where I_h is a constant, set by the initial conditions. (A constant current of zero also satisfies it.) This solution describes an unforced time evolution of the resonator voltage, which decays at an exponential rate of 2τ. This corresponds to a stored energy decay time of τ.

Now we combine the homogeneous and inhomogeneous solutions to match the turn-on, steady state and decay of the voltage on the resonator. We choose the following two solutions to represent first the buildup of the voltage from zero to a steady state and second to represent the decay of the voltage from the driven steady state following the turning off the drive:

Eq. 5.5a $$I = I_i\left(1 - e^{-t/2\tau}\right)$$

Eq. 5.5b $$I = I_i e^{-t/2\tau}$$

Here I_i is taken from Eq. 5.4. By using the same function I_i for both solutions, we insure a match between the steady state solution of the inhomogeneous equation and the initial value for the power turn-off phase of the homogeneous equation.

We have interest in two cases: First, the transient when the resonator starts from zero voltage and the buildup of voltage towards the steady state, and in particular the reflected power at the instant of turn-on and at the steady state in terms of the forward power. The second case of interest is the decay of the voltage when the driving forward current is turned off, and in particular the reflected power at the instant of the turn-off.

For the buildup of the resonator current to steady state we use Eq. 5.5a:

Eq. 5.6 $$I = \frac{2\beta I_f}{1+\beta}\frac{1-e^{-t/2\tau}}{1+j\delta}$$

It must be remembered that these currents are measured on the resonator side of the transformer. At the power source side the currents are reduced by a factor of n.

The decay of the stored energy of the resonator (the solution of the homogeneous equation) is straightforward; we square the time dependence of the current of the homogeneous solution:

$$U = U_0 e^{-t/\tau}$$

Next we would like to get the reflected current when the forward current is turned on. We substitute Eq. 5.6 into Eq. 5.2, and get

$$I_f - I_r = \frac{2\beta I_f}{1+\beta}\frac{1-e^{-t/2\tau}}{1+j\delta}$$

Collecting terms we obtain the solution for the reflected current

Eq. 5.7 $$I_r = I_f\left[1 - \frac{2\beta}{1+\beta}\frac{1-e^{-t/2\tau}}{1+j\delta}\right]$$

Equation Eq. 5.7 has some important specific limits. At t=0 (forward pulse just turned on), the full forward current is reflected (regardless of the frequency). At steady-state, $t = \infty$, and on resonance, $\delta = 0$, we get

Eq. 5.7a $$I_r = I_f \frac{1-\beta}{1+\beta}$$

The reflection coefficient is another important consequence of Eq. 5.7. It is defined as the ratio of the reflected voltage to the forward voltage.

Eq. 5.7b $$\Gamma \equiv \frac{V_r}{V_f} = \frac{I_r}{I_f} = 1 - \frac{2\beta}{1+\beta}\frac{1-e^{-t/2\tau}}{1+j\delta}$$

The reflected power on resonance ($\delta = 0$) is given in terms of the forward power:

Eq. 5.7c $$P_r = P_f \left(1 - \frac{2\beta}{1+\beta}\left(1 - e^{-t/2\tau}\right)\right)^2$$

The steady-state ($t = \infty$) reflected power is given by:

Eq. 5.7d $$P_r = P_f \left(\frac{1-\beta}{1+\beta}\right)^2$$

The resonator voltage can be expressed in terms of the forward current:

Eq. 5.8 $$V = 2ZI_f \left[1 - \frac{\beta}{1+\beta}\frac{1-e^{-t/2\tau}}{1+j\delta}\right]$$

We can get the resonator's stored energy from the current in the inductor:

Eq. 5.9 $$U = LII^* = \frac{4\beta P_f \tau}{1+\beta}\frac{1}{1+\delta^2}\left(1 - e^{-t/2\tau}\right)^2$$

It is zero at t=0, and at the steady state (t=∞) we get

Eq. 5.9a $$U = \frac{4\beta P_f \tau}{1+\beta}\frac{1}{1+\delta^2}$$

The power turn-off is also interesting; we would like to know the value of the reflected current (power) on resonance and at the instant the forward power is turned off, which is when the pulse reached steady-state:

$$I = I_{f0}\frac{2\beta}{1+\beta}$$

Now we switch of the forward power, I_f=0, at this instant we get $I_r = I$, the reverse current is just the resonator's steady-state current.

Thus we obtain

Eq. 5.10 $$I_r = I_{f0}\frac{2\beta}{1+\beta}$$

The power sent by the resonator into the transmission line, on resonance and just as the forward power was turned off is then:

Eq. 5.10a $$P_r = P_{f0}\frac{4\beta^2}{(\beta+1)^2}$$

5.2 The determination of β through the reflected power port

The reflected power as a function of time, following a sudden switch-on of the forward power, is shown in Figure 2. Here we use the following expressions developed above in Section 5.1. In particular we want to measure the reflected power (obtained by squaring the reflected voltage) at the three sampling points, 'a', 'b' and 'c', where 'a' is just at the forward power turn-on (showing full reflection from the empty cavity), 'b' is just before the end of the forward power pulse (where saturation of the reflected power is achieved), and 'c' is just as the forward power was turned off (measuring the power transmitted back from the cavity through the FPC).

Thus, at time t = 0, we obtain from Eq. 5.7c that

$$P_a = P_f$$

Then, Eq. 5.7d tells us that

$$P_b = P_f\left(\frac{1-\beta}{1+\beta}\right)^2$$

Finally, we learn from Eq. 5.2 that when the forward current is turned off, the reflected current equals the steady-state resonator current, which we take from Eq. 5.4. Then we square the currents to obtain the power, and thus we establish:

$$P_c = P_f\frac{4\beta^2}{(1+\beta)^2}$$

Therefore, it follows from the definitions by simple algebra that:

$$\beta = \frac{P_c}{P_a - P_b}$$

This is correct as long as we can neglect the coupling of the transmitted power antenna. Recognizing that P_a-P_b represents the power sent to both the cavity losses and the transmitted power, we can write

$$\beta \equiv \frac{Q_0}{Q_e} = \frac{\boldsymbol{P_e}}{\boldsymbol{P_f - P_r - P_t}}$$

where we continue with the convention that bold faced variables represent the correct absolute power levels. Since we want to do away with absolute power measurements with the exception of the forward and transmitted power, we substitute the emitted power from the FPC, $\boldsymbol{P_e}$ and the reflected power $\boldsymbol{P_r}$ by

$$\boldsymbol{P_e} = \boldsymbol{P_f}\frac{P_c}{P_a}$$

and

$$\boldsymbol{P_r} = \boldsymbol{P_f}\frac{P_b}{P_a}$$

and then we get for β the desired expression in terms of the measured variables that uses just ratios of quantities measured in the reflected power port and the two absolute power measurements, the forward and transmitted power, making this a robust measurement:

$$\beta = \frac{P_c}{P_a(1-\epsilon) - P_b}$$

where

$$\epsilon \equiv \left|\boldsymbol{P_t}/\boldsymbol{P_f}\right|$$

and we can reduce β_t in exactly the same manner to

$$\beta_t \equiv \frac{Q_0}{Q_t} = \frac{\boldsymbol{P_t}}{\boldsymbol{P_f} - \boldsymbol{P_r} - \boldsymbol{P_t}}$$

which yields the desired expression of β_t in terms of the measured variables:

$$\beta_t = \epsilon\frac{P_a}{P_a(1-\epsilon) - P_b} = \beta\epsilon\frac{P_a}{P_c}$$

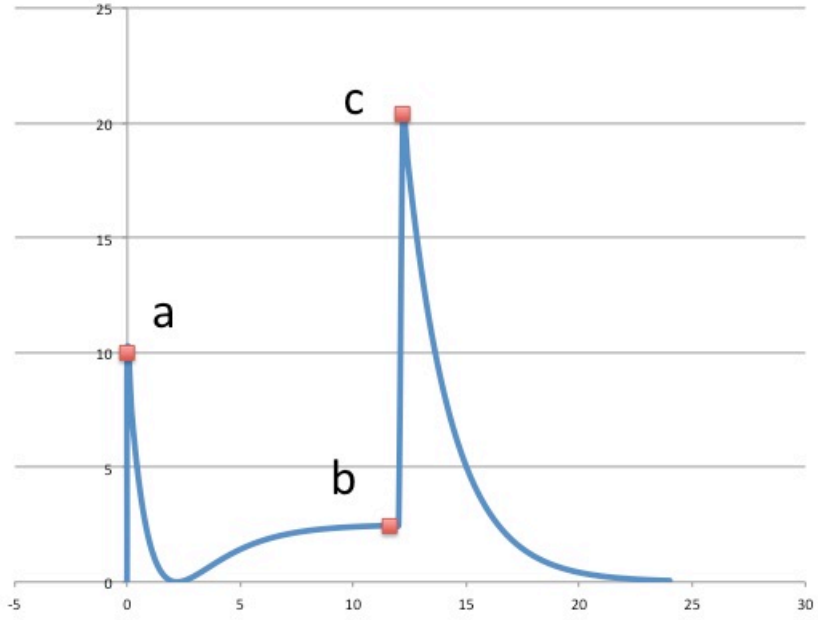

Figure 2. The reflected power as a function of time (in units of the decay time τ) for $P_f = 10$ and $\beta = 3$. The forward power is turned on at $t/\tau = 0$ and off at $t/\tau = 12$. The red squares designate the three sampling points, 'a', 'b' and 'c', (from left to right) where 'a' is just at the forward power turn-on (showing full reflection from the empty cavity), 'b' is just before the end of the forward power pulse (where saturation of the reflected power is achieved), and 'c' is just as the forward power was turned off (measuring the power transmitted back from the FPC).

5.3 Methods used in the CW scan.

In the CW scan, our objective is to obtain the loaded Q of the cavity without having access to the decay time. We also would like to monitor the correct setting of the loop-phase, to avoid errors introduced by a phase drift. We can do this by considering the detuning the loop phase shift by a small amount and observing the corresponding changes of the cavity's frequency and amplitude.

The observable we use is the transmitted voltage V_t from the pickup antenna, which includes information about the cavity's amplitude and phase. This voltage is just proportional to the resonator's current, which we have from Eq. 5.6. We are interested just in the relative dependence on frequency, at steady state. Thus, we write

$$V_t = V_t^0 \frac{1}{1 + j\delta}$$

At a small phase value of $\delta = Q_L\Delta$, the phase can be approximated as $\varphi \approx -Q_L\Delta$, so the phase dependence on frequency near resonance is

$$\varphi \approx -\frac{2Q_L(\omega_0 - \omega)}{\omega_0}$$

The transmitted voltage amplitude varies as

$$V_t(\delta) \approx V_t^0(1 - \delta^2) \approx V_t^0(1 - \varphi^2)$$

Note that the modulation does not have to be small; we can use the exact expressions and get accurate results. However, we do not want a large modulation of the stored energy in order to minimize the change in Q as a function of the resonator's voltage over the range of the measurement.

The amount of frequency modulation per small phase change yields the loaded Q of the cavity

$$Q_L = -\frac{\varphi}{\Delta} \approx -\frac{\varphi\omega_0}{2(\omega_0 - \omega_1)}$$

where $\omega_1$is the new frequency. Thus, we obtained a measurement of Q_L (or τ) without having to measure τ directly.

This procedure assumes that enough time has been allowed for the SEL to achieve its new frequency following the step in the loop-phase. This can be quite time consuming for a superconducting cavity. Therefore, we observe that following a loop-phase change, the voltage of the cavity at the original frequency ω_0 starts decaying according to the homogeneous solution as

$$V_t(\omega_0, t) = V_t^0(\omega_0)e^{-t/2\tau}$$

and the voltage at the new frequency starts building up as

$$V_t(\omega_1, t) = V_t^0(\omega_1)\left(1 - e^{-t/2\tau}\right)$$

The amplitude of the transmitted voltages at both frequencies will be equal at a time t such that

$$\left(1 - e^{-t/2\tau}\right) = e^{-t/2\tau}$$

This time is

$$t = 2\tau ln2 \approx 1.386\tau$$

At this time the observed frequency of the cavity will be

$$\omega = \frac{\omega_0 + \omega_1}{2}$$

However, the purpose of this measurement is to establish τ. Thus, we have to solve this in a self-consistent method. To do this, we track the frequency output $\omega(t)$ from the SEL as a function of time t from the application of the phase jump φ. At some point t_1 in time the following equation will be satisfied by the measured frequency ω_1:

$$\omega_1 - \omega_0 = -\frac{1.386\varphi}{2t_1}$$

At this point we have established a self-consistent value for τ

$$\tau = \frac{t_1}{2ln2}$$

Next let us look at the correct setting of the loop-phase. Let us assume that the loop-phase is not set right by a small amount θ. It follows that the amplitude of the cavity's transmitted voltage will have an asymmetric shift when we apply steps ±φ in the loop phase:

$$V_t(\varphi) \approx V_t^0(1-\varphi^2)$$

$$V_t^+ = V_t^0[1-(\vartheta+\varphi)^2]$$

in the positive phase swing direction, and

$$V_t^- = V_t^0[1-(\vartheta-\varphi)^2]$$

in the negative phase swing direction.

Therefore, we obtain the phase offset as

$$\vartheta = -\frac{1}{2\varphi}\frac{V_t^+ - V_t^-}{V_t^+ + V_t^-}$$

ϑ may be then applied as a change to the loop-phase to restore the correct value.

5.4 Error analysis

It is important to estimate well the experimental error of the measured cavity parameters; in particular the stored energy U and the intrinsic quality factor Q_0. These errors depend in turn on errors of intermediate variables, such as the coupling coefficient β. We denote errors in a variable by the sign ∂.

The errors can be classified by calibration errors, where we are interested in the errors on Q_e and Q_t, (which are then used in scans) and scan errors where we are interested in the errors on U and Q_0. The pulsed scan and the CW scan have slightly different errors in Q_0.

Furthermore, we can classify the errors as statistical or systematic. The sources of random statistical errors are derived from the digitization noise in the FPGA board DACs. There are many sources of systematic errors: Some are associated with equipment, such as cable attenuation errors; directional coupler isolation; and circulator coupled-port reflection. Others are associated with incorrect operation of the SEL, such as too short cavity filling or emptying times or incorrect loops phase. Systematic errors are directional.

5.4.1 Statistical errors

Statistical errors are derived from digitization noise and can be minimized by a prudent choice of the ADC word size, by a careful selection of the attenuations in the path to the SEL board, including the coupling strength of the directional coupler. Since the SEL board takes measurements at a very high rate and includes averaging, it can also calculate the statistical error on any of the measured variables, that is in τ, P_a, P_b, P_c, $\mathbf{P_f}$ and $\mathbf{P_t}$.

5.4.1.1 Decay time τ error

The decay time τ is measured by a best-fit procedure to a decay of the stored energy as described in the calibration section. Thus the error is given by the software procedure as a measured value of $\partial\tau/\tau$

5.4.1.2 Coupling coefficient error

The coupling coefficient is obtained from the expression

$$\beta = \frac{P_c}{P_a - P_b}$$

where P_a, P_b and P_c are digitized from the reflected power port of the directional coupler at particular times marked by the points 'a', 'b' and 'c' as defined in Figure 2 (Section 5.1). We neglect the transmitted power in this error analysis, since it is small and its error is negligible.

Since all three variables P_a, P_b and P_c are measured in the same circuit of the reflected power port of the directional coupler, the statistical noise contributing to $\partial\beta$ is the ADC noise, which is provided by the FPGA board as statistical errors:

$$\partial P_{Na};\ \partial P_{Nb};\ \partial P_{Nc}$$

Therefore, the statistical contribution to the error in β is given by

$$\frac{\partial\beta_N}{\beta} = -\frac{\partial P_{Na}}{P_a - P_b} + \frac{\partial P_{Nb}}{P_a - P_b} + \frac{\partial P_{Nc}}{P_c}$$

Clearly the errors in P_a and P_b are magnified by coefficients that can be large for a coupling that is far from critical. This is why it is important to read them from the same port of the directional coupler, and it also points to the advantage of a variable coupler in error reduction.

5.4.2 Systematic equipment errors

In this section we treat errors stemming from cable calibration and from the directional coupler and circulator.

5.4.2.1 Forward power P_f error

The actual forward power impinging on the cavity's FPC is given (see Section 2.1 above) by

$$\boldsymbol{P_f} = \frac{W_f^2}{N} 10^{0.1(A_{f1} - A_{f2})}$$

Let us address the cable attenuation errors as an aggregate; defining $A_f=A_{f1}-A_{f2}$, and designating the total forward power cable attenuation error as ∂A_f
Thus we can write

$$\frac{\partial \boldsymbol{P_f}}{\boldsymbol{P_f}} = 0.23\partial A_f$$

The statistical error $\partial \mathbf{P_f}/\mathbf{P_f} = 2\,\partial W_f/W_f$ has to be added to the systematic error calculated here.
Where the first term is the ADC noise, which should be negligible with the proper choice of the magnitude of W_f, and the second term represents the error in the forward power cable calibration now taken in dB.

5.4.2.2 Transmitted power P_t error

The actual power transmitted from the field antenna, $\mathbf{P_t}$, is obtained from

$$\boldsymbol{P_t} = \frac{W_t^2}{N} 10^{0.1A_t}$$

Thus in similarity to the forward power error above,

$$\frac{\partial \boldsymbol{P_t}}{\boldsymbol{P_t}} = 0.23\partial A_t$$

Where ∂A_t is the transmitted power cable calibration error in dB.

5.4.2.3 Directional coupler isolation errors

The isolation I_r of the reflected power port of a directional coupler, not being infinite, introduces a fraction of the forward power passing through the directional coupler into the reflected power port. Thus an error is introduced into the measurement of the reflected power. Since the phase of this signal depends on the exact length of cables between the directional coupler and the cavity, it is not possible to state the exact error but place an upper bound on it. Similarly, a good (large negative number) isolation I_f of the forward power port is necessary to prevent the reflected power from the cavity to introduce an error in the measurement of the forward power.

Since the signal mixing in the ports of the directional coupler takes place by adding voltages, it is important that the isolation is calculated as a voltage. If the isolation is given in a certain value of dB of power, say a 40 dB power isolation (which may look good) it has to be converted to voltage. For this example, the isolation in voltage is now only 20 dBV. Thus, in the following we will use the isolation in dBV.

Therefore, for all of the variables, P_a, P_b and P_c measured on the reflected power port of the directional coupler, we must add an error related to the isolation quality:

$$\frac{\partial V_{Ix}}{V_a} = 10^{0.1I_r}$$

$$\frac{\partial P_{Ix}}{P_a} = 2 \cdot 10^{0.1I_r}$$

where ‘x‘ stands for ‘a’, ‘b’ or ‘c’, and I_r is the isolation in dBV.

This error can be serious unless a high-quality directional coupler is used. For example, in order to obtain a fractional error in power of 1%, the directivity of the directional coupler has to be about 46 dB [3].

5.4.2.4 Circulator coupled port match error

The reflection of power C_f from the coupled port of the circulator (the port connected to the directional coupler) measured as a S_{22} voltage ratio in dBV sends a fraction of the reflected power from the cavity in the forward direction, introducing and error in the forward power measurement. Again, it is the voltage error that adds, and the phase depends on the length of cables, but we can state an upper limit on the error.

$$\frac{\partial P_{Cf}}{P_f} = 2 \cdot 10^{0.1C_f}$$

Here as in the previous section *Cf* is in dBV. This error can be serious unless a high-quality circulator is used. A possible (but expensive) method to reduce this error is to add a high-quality power (low VSWR) attenuator directly after the circulator. If the attenuation is A, then the error signal passes the attenuator three times. Thus, the power amplifier has to have $10^{0.2A}$ higher power, but the voltage reflection coefficient has been improved by 3A.

5.4.3 Systematic operational errors

Systematic operation errors are of two types: Cavity fill errors and loop-phase errors.

5.4.3.1 Fill errors

There are two types of cavity fill errors to assess.

The first fill error is caused by too-short power-on pulse. Let us denote to power on pulse time by t_p. In this case we encounter errors in both P_b and P_c, but not in Pa.

From Section 5.1 Eq. 5.7c we got (on resonance):

$$P_r = P_f \left(1 - \frac{2\beta}{1+\beta}\left(1 - e^{-t/2\tau}\right)\right)^2$$

Our derivation of β uses P_b based on $e^{-t/2\tau} = 0$ in the expression for the reflected power after turn-on, yielding

$$P_b = P_a \left[\frac{1-\beta}{1+\beta}\right]^2$$

However, for a finite pulse t_p we get instead

$$P_b = P_a\left(1 - \frac{2\beta}{1+\beta}\left(1 - e^{-t_p/2\tau}\right)\right)^2$$

which can be rewritten after some algebra as

$$P_b = P_a\left[\frac{1-\beta}{1+\beta}\right]^2\left(1 + \frac{4\beta}{(1-\beta)}e^{-t_p/2\tau}\right)$$

Now, to get the difference from the expected value of P_b, we subtract:

$$\frac{\partial P_b}{P_a} = \left[\frac{1-\beta}{1+\beta}\right]^2 - \left[\frac{1-\beta}{1+\beta}\right]^2\left(1 + \frac{4\beta}{(1-\beta)}e^{-t_p/2\tau}\right)$$

Thus the error is

$$\frac{\partial P_{Fb}}{P_a} = -4\frac{\beta(1-\beta)}{(1+\beta)^2}e^{-t_p/2\tau}$$

The direction of this error depends on β, it increases the value of P_b for β<1, and decreases it for β>1.

The error in P_c is simply evaluated as a cavity that has been filled to a lower value than planned, thus it decreases P_c

$$\frac{\partial P_{Fc}}{P_a} = -\frac{4\beta^2}{(1+\beta)^2}e^{-t_p/\tau}$$

In order to make this error as small as 1% regardless of the value of β, the pulse length t_p should be over 9 decay times! However, for a well-matched FPC (β about 1) the error in P_b becomes small.

The second fill error is to have a finite stored energy at the beginning of the forward-power-on pulse. This can be caused by either waiting a time too short between two pulses or by the pedestal encountered by the turn-on of the pulse. This will lead to an erroneous value of P_a.

Let's assign the energy already stored at the cavity the variable U_i. To obtain the reflected power at the moment we step up the forward power, we use

$$P_r = P_f - P = P_f - \frac{U_i\omega}{Q_0}$$

Clearly when U_i=0, then all the power is reflected. Therefore, the error in P_a is

$$\partial P_{Fa} = -\frac{U_i\omega}{Q}$$

To evaluate U_i, we consider two cases. One is that we waited too short a time for the cavity to empty from the previous pulse. The other is the pedestal used to get the SEL to oscillate at low power before stepping up the forward power. Let us first dismiss the first case: There is no reason why one should not wait a sufficient time after a powered cavity to send a calibration pulse. Just for completeness we observe

that if the cavity was powered to a level U at a time t_w before the calibration pulse, this results in a value for U_i that is simply:

$$U_i = Ue^{-t_w/\tau}$$

Thus about 15 decay times of waiting should bring this error down to the 10^{-3} level.

For the remaining case of a start pedestal, let us assume that we use a voltage that is ε times smaller than the intended calibration pulse forward voltage, and we apply this pedestal for a time t_i. Taking the conservative assumption that for all this time the cavity has been filling, we find that U_i, the stored energy filled during the pedestal, on resonance, is found by using Eq. 5.9

$$U_i = \frac{4\varepsilon^2\beta P_f\tau}{1+\beta}\left(1-e^{-t_i/2\tau}\right)^2 \approx \frac{\beta P_f}{\tau(1+\beta)}\varepsilon^2 t_i^2$$

therefore

$$\partial P_{Fa} = -\frac{\beta P_f}{\tau^2(1+\beta)^2}\varepsilon^2 t_i^2$$

$$\frac{\partial P_{Fa}}{P_a} = -\frac{\beta}{(1+\beta)^2}\varepsilon^2\left(\frac{t_i}{\tau}\right)^2$$

Now we have established the complete expression for the fill error in β, in the order of contributions from P_a, P_b and P_c:

$$\frac{\partial\beta_F}{\beta} = -\frac{P_a}{P_a-P_b}\left[\frac{\beta}{(1+\beta)^2}\varepsilon^2\left(\frac{t_i}{\tau}\right)^2\right] - \frac{P_b}{P_a-P_b}\left[\frac{4\beta(1-\beta)}{(1+\beta)^2}e^{-t_p/2\tau}\right] - \frac{4\beta^2}{(1+\beta)^2}e^{-\frac{t_p}{\tau}}$$

Note that all the errors in the signals from the reflected power port lead to a smaller apparent value of β.

5.4.3.2 Loop phase error

The reflection coefficient Γ of the cavity's FPC port depends on the loop-phase through the change it induces in the frequency (see derivation in Section 5.1), so we use Eq. 5.7b at steady-state

$$\Gamma = 1 - \frac{2\beta}{1+\beta}\frac{1}{1+j\delta}$$

And we set $\delta = -\vartheta$

$$\Gamma = 1 - \frac{2\beta}{1+\beta}\frac{1}{1-j\vartheta}$$

This in turn leads to a new value of the reflected power:

$$P_r = P_f \Gamma\Gamma^* = P_f \left[\left(\frac{\beta - 1}{\beta + 1} \right)^2 + \frac{4\beta^2 \vartheta^2}{(\beta + 1)^2} \right]$$

Clearly, where $\vartheta=0$ we get the ratio of the reflected power to the forward power derived in Section 5.1. Therefore the error in P_r (or P_b) is just

$$\frac{\partial P_b}{P_a} = \frac{4\beta^2 \vartheta^2}{(\beta + 1)^2}$$

It is quadratic in ϑ and furthermore, given that the loop-phase is continuously checked it is negligible. A similar argument follows for phase errors in P_a and P_c.

5.4.4 Calibration error estimates

The products of the calibration sequence are just the two external coupling coefficients, Q_e and Q_t. In the error analysis we neglect β_t against β. Then we obtain from Section 3.2 the following equations (again, the transmitted power is neglected here):

$$Q_e = \frac{1 + \beta}{\beta} \omega\tau$$

and

$$Q_t = \frac{1 + \beta}{\beta_t} \omega\tau$$

as well as the following

$$\beta_t = \beta \frac{\boldsymbol{P_t}}{\boldsymbol{P_f}} \frac{P_a}{P_c}$$

Thus we get the errors:

$$\frac{\partial Q_E}{Q_E} = \frac{1 + \beta}{\beta^2} \frac{\partial \beta}{\beta} + \frac{\partial \tau}{\tau}$$

$$\frac{\partial \beta_t}{\beta_t} = \frac{\partial \beta}{\beta} + \frac{\partial \boldsymbol{P_t}}{\boldsymbol{P_t}} - \frac{\partial \boldsymbol{P_f}}{\boldsymbol{P_f}} + \frac{\partial P_a}{P_a} - \frac{\partial P_c}{P_c}$$

$$\frac{\partial Q_t}{Q_t} = \frac{\partial \beta}{\beta} - \frac{\partial \beta_t}{\beta_t} + \frac{\partial \tau}{\tau}$$

In order to avoid tediously long expressions, we will not substitute the values of the errors of the variables used here since these are all available above.

5.4.5 Scan error estimates

In a pulsed scan, we derive Q_0 through the expression

$$Q_0 = Q_L(1 + \beta) = \omega\tau(1 + \beta)$$

ω is known quite precisely, thus assuming no correlation between errors in τ and β,

$$\frac{\partial Q_0}{Q_0} = \frac{\partial \tau}{\tau} + \frac{\partial \beta}{1+\beta}$$

We derive U through the expression

$$U = K\boldsymbol{P_t} = \frac{Q_t}{\omega}\boldsymbol{P_t}$$

Thus

$$\frac{\partial U}{U} = \frac{\partial Q_t}{Q_t} + \frac{\partial \boldsymbol{P_t}}{\boldsymbol{P_t}}$$

In a CW scan, the error in U is the same as for the pulsed scan above, but instead of using the decay τ, we use the phase modulation to determine Q_L.

We determine Q_L from

$$Q_L = \frac{f\varphi}{2\delta_f}$$

Since f and φ are exact values, the error is simply

$$\frac{\partial Q_L}{Q_L} = -\frac{\partial \delta_f}{\delta_f}$$

and this is a purely statistical error to be evaluated by the board.

5.5 GUI and data recording.

5.5.1 Parameters to be set by user

1. Target frequency f. Set the angular frequency ω = 2πf.
2. Cavity forward power.
3. Maximum allowable power (alarm if forward power exceeds maximum allowable power).
4. For all scan modes, initial power, final power and number of steps.
5. Pulsed scan:
    a. Pulse width, minimum 0.5 mSec.
    b. Period, minimum equal to pulse width.
    c. Number of pulses (including a continuous option)
6. CW scan:
    a. Phase modulation value Φ
    b. Phase modulation angular frequency Ω
    c. Integration periods, related to integration time in units of 2π/Ω
7. Calibration factors:
    a. Factor converting ADC number to power at the terminal.
    b. Attenuation in dB of forward, reflected and transmitted powers.
    c. Gain in amplifier chain for sending power to the cavity, in dB.
8. Cavity property κ relating stored energy to voltage (or gradient) squared.

9. [Set amplitude for feed-back; future only.]
10. Parameter of interest is voltage or gradient.
11. Maximum radiation level.
12. Maximum cavity vacuum.

5.5.2 User Controls

1. Calibration, phase adjustment, conditioning, pulsed scan or CW scan mode selector.
2. Power on/off
3. Start sequence.
4. [Amplitude lock on / off; future only]
5. [Phase lock on / off; future only]

5.5.3 Readout data on display

1. Reproduce all the set and control parameters mentioned above in Sections 5.4.1 and 5.4.2.
2. Frequency at pulse start (low stored energy), at pulse end and the derived Lorentz detuning factor.
3. Frequency error noise, frequency error spectrum.
4. Forward power P_f, at sample point (b) in units of watts.
5. Reflected power P_a, P_b, Pc at sample point (a), (b), (c) and transmitted power P_t at (d). All units are watts (calibrations have to be used).
6. Reflected and emitted power vs. time curves, indicating location of sample points. Units are watts.
7. Decay time of emitted power, in seconds.
8. Quality of fit for decay curve.
9. Calculated Field (or voltage), MV or MV/m and its error
10. Calculated Q_0 and its error. Units of 10^9
11. Calculated coupling factor $\beta = (Q_0/Q_e)$
12. Calculated Q_e, the external Q of the FPC, units of 10^9.
13. Calculated Q_t, the external Q of the pickup probe, units of 10^9.
14. Calculated cavity dissipated power in watts.
15. Calculated stored energy (Joules).
16. Radiation level [environmental variable].
17. Vacuum in cavity [environmental variable].
18. Cavity temperature (multiple points) [environmental variables].
19. Liquid helium levels, [environmental variables].
20. Cryostat pressure [environmental variable].
21. Error indicators: τ fit, over-power in forward, out of amplitude lock, out of phase lock, over limit for radiation, over limit for cavity vacuum.

6 References

[1] Theory and practice of cavity rf test systems, Tom Powers, Proceedings of the 12th International Workshop on RF Superconductivity, Cornell University, Ithaca, New York, USA, 2006
[2] RF Superconductivity for Accelerators, H. Padamsee, J. Knobloch, T. Hays, John Wiley & Sons New York 1988
[3] Nikolai Schwerg, private communication August 16, 2017.

7 Acknowledgements

IBZ would like to thank the CERN BE-RF group for its hospitality and the stimulation to work on this subject, including Rama Calaga, Erk Jensen, Karl-Martin Schirm and in particular the hospitality of Alick Macpherson and his team. Special thanks go to Karim Gibran Hernandez Chahin, Nicholas Shipman and Nikolai Schwerg for critical reading of the document and excellent suggestions for improvements.